Sains Malaysiana 52(12)(2023): 3533-3550
http://doi.org/10.17576/jsm-2023-5212-15

Pyranocycloartobiloxanthone A Suppressed Metastasis Ovarian Cancer Cells via S Phase Cell Cycle Arrest and Apoptosis

(Piranosikloartobilozanton A Menindas Metastasis Sel Kanser Ovari melalui Hentian Kitaran Sel Fasa S dan Apoptosis)

MASHITOH ABD RAHMAN[1], NAJIHAH MOHD HASHIM[1,2,*] & IDRIS ADEWALE AHMED[3]

[1]*Department of Pharmaceutical Chemistry, Faculty of Pharmacy, Universiti Malaya, 50603 Kuala Lumpur, Malaysia*
[2]*Centre for Natural Products Research and Drug Discovery (CENAR), Universiti Malaya, 50603 Kuala Lumpur, Malaysia*
[3]*Department of Biotechnology, Faculty of Applied Science, Lincoln University, Kelana Jaya 47301 Petaling Jaya, Selangor, Malaysia*

Received: 14 April 2023/Accepted: 11 December 2023

ABSTRACT

Ovarian cancer is a deadly disease with a poor prognosis, highlighting the urgent need for novel therapeutic alternatives. Pyranocycloartobiloxanthone A (PA), an exceptional xanthone compound has garnered attention due to its diverse medicinal properties. This study aimed to investigate the anticancer properties of PA on metastatic ovarian cancer SKOV-3 cells. Cytotoxicity was evaluated using an MTT assay, while apoptotic mechanisms were determined using AO/PI double staining, annexin V-fluorescein isothiocyanate, multiple cytotoxicity-3, reactive oxygen species (ROS) production, caspases, real-time PCR, western blot, human apoptosis protein profile array and cell cycle analysis. PA inhibited SKOV-3 cell proliferation in a time-dependent manner, with an IC_{50} of 7.0 ± 0.5 µg/mL and a selectivity index of 13.2 after 72 h of treatment. PA induced apoptosis through the intrinsic apoptotic pathway and arrested the cell cycle at the S phase. PA stimulated ROS production and disrupted the mitochondrial membrane potential, releasing cytochrome *c* from mitochondria to the cytosol. Additionally, results from human apoptotic protein profile indicated that 21 proteins were upregulated while 22 proteins were downregulated, including Bcl-2, survivin, and HSP70. These findings suggest that PA has the potential as a lead molecule in the development of a chemotherapy drug for ovarian cancer. However, further research is necessary to evaluate the safety and efficacy of PA in preclinical and clinical settings.

Keywords: Apoptosis; *Artocarpus obtusus*; cell cycle; ovarian cancer; pyranocycloartobiloxanthone A

ABSTRAK

Kanser ovari adalah penyakit yang membawa maut dengan prognosis yang kurang baik, menunjukkan keperluan yang mendesak untuk terapi alternatif yang novel. Piranosikloartobilozanton A (PA), sebatian zanton yang luar biasa telah menarik perhatian kerana sifat perubatannya yang pelbagai. Penyelidikan ini bertujuan untuk mengkaji sifat antikanser PA ke atas sel kanser ovari metastatis SKOV-3. Sitotoksisiti dinilai menggunakan asai MTT, manakala mekanisme apoptosis ditentukan menggunakan pewarnaan berganda AO/PI, annexin V-fluoresein isotiosianat, pelbagai sitotoksisiti-3, pengeluaran spesies oksigen reaktif (ROS), *caspases*, masa nyata PCR, pemblotan western, profil protein apoptosis manusia dan analisis kitaran sel. PA merencat proliferasi sel SKOV-3 bergantung kepada masa dengan IC_{50} 7.0 ± 0.5 µg/mL dan indeks selektiviti sebanyak 13.2 selepas 72 jam rawatan. PA aruhan apoptosis melalui laluan apoptosis intrinsik dan menahan kitaran sel pada fasa S. PA merangsang pengeluaran ROS dan mengganggu potensi membran mitokondria, melepaskan sitokrom *c* daripada mitokondria ke sitosol. Selain itu, hasil daripada profil protein apoptosis manusia menunjukkan bahawa pengawalaturan 21 protein telah meningkat manakala 22 protein telah menurun termasuk Bcl-2, survivin dan HSP70. Penemuan ini mencadangkan bahawa PA mempunyai potensi sebagai molekul utama dalam membangunkan dadah kemoterapi untuk kanser ovari. Walau bagaimanapun, kajian lanjut adalah perlu untuk menilai keselamatan dan keberkesanan PA dalam konteks praklinikal dan klinikal.

Kata kunci: Apoptosis; *Artocarpus obtusus*; kanser ovari; kitaran sel; piranosikloartobilozanton A

Introduction

Ovarian cancer is currently the most fatal gynaecological cancer with a global report of 313,959 new cases and 207,252 deaths in 2020 alone, thus, assuming the fourth most common cause of female cancer (Joly et al. 2022; Marchetti et al. 2021). Furthermore, only a small portion of ovarian malignancies originates from the sex-cord stromal tissues or germ cells whereas the vast majority (90%) of them are of epithelial origin and thus, are referred to as epithelial ovarian cancer (EOC) (Maleki et al. 2022; Schoutrop et al. 2022). The other common EOC histological subtypes include clear cell, endometrioid, mucinous, and low-grade or high-grade serous carcinomas (Ivanova, Dikov & Dimitrova 2017). Though the cumulative mortality risk of ovarian cancer is almost similar worldwide, its incidence in more developed countries is twice as high compared to developing countries (Marchetti et al. 2021).

Ovarian cancer is notorious for its asymptomatic early stages, making it challenging to detect until it reaches advanced disease stages, often classified as stage III and IV according to International Federation of Gynaecology and Obstetrics (FIGO) (Pellegrini et al. 2022). By the time many cases are diagnosed, the cancer has already spread extensively within the abdominal cavity or to distant sites. Cytoreductive surgery (extensive debulking) followed by platinum-based adjuvant chemotherapy with or without maintenance therapy (such as poly adenosine diphosphate ribose polymerase [PARP] inhibitors or angiogenesis inhibitor bevacizumab) are the mainstay and gold standard of ovarian cancer first-line therapy (Wu et al. 2021). However, in many cases, despite the initial treatment regimen, patients with epithelial ovarian cancer (EOC) face a grim 5-year survival rate of 46%, with recurrence and metastasis being common outcomes due to the limited effectiveness of adjuvant chemotherapy following cytoreductive surgery (Wang et al. 2022).

Metastasis in ovarian cancer typically occurs through three primary routes: transcoelomic, hematogenous, or lymphatic dissemination (Pal et al. 2023; Yeung et al. 2015). These pathways allow cancer cells to break free from the ovaries or fallopian tubes, leading to the formation of extensive tumours that can spread beyond the abdominal cavity. This advanced stage of cancer is often associated with a bleaker prognosis and a higher mortality rate compared to cancers that remain localized. This stark reality underscores the urgent need for more effective treatment strategies to combat the metastatic nature of the disease and overcome the challenges posed by late-stage diagnosis and chemotherapy resistance.

Apoptosis, the controlled process of cell death, is intricately regulated by two main pathways: the extrinsic pathway, which responds to external signals via cell surface death receptors, and the intrinsic pathway, initiated by genotoxic stress and involving mitochondrial mediation. These pathways harmonize the action of numerous proteins, including members of the BCL-2 family (Singh & Lim 2022). Any disruption or malfunction in this intricate network can result in cancer cells successfully evading apoptosis, posing a challenge in cancer therapy. Therefore, the development of an efficient cancer chemotherapeutics strategy requires an understanding of the apoptosis pathways. On the other hand, a new horizon to treat cancer is the exploration of natural products and compounds derived from medicinal plants owing to their potential to be used in combination with chemotherapy drugs to improve their efficiency (Gielecińska et al. 2023; Smirnova et al. 2022).

Artocarpus obtusus Jarrett (Family Moraceae) locally known as 'pala tupai' is an endemic species of Borneo mostly growing in lowland and freshwater swamp forests both in the tropical and subtropical regions (Sidahmed et al. 2013). Pyranocycloartobiloxanthone A (PA) (Figure 1) is a new xanthone and a major bioactive compound that was first isolated from *A. obtusus* (Hashim et al. 2010). Other studies, however, have shown that PA can be isolated from *A. anisophyllus* (Lathiff et al. 2015) and *A. hirsutus* (Nayak et al. 2018). PA has cytotoxic and antiproliferative effects in MCF7 cells through NF-kB and Bcl2/Bax signaling pathways (Hashim et al. 2012; Mohan et al. 2012), in addition to other diverse range of biological activities such as strong antimicrobial, free radical scavenging, anti-tyrosinase inhibitory, gastroprotective activity, and anti-acne activities (Hashim et al. 2012; Nayak et al. 2018; Sidahmed et al. 2013). Though PA has been shown to have antiproliferative effects on several cancer cell lines, its effects on metastatic ovarian cancer SKOV-3 cells, however, have yet to be evaluated. Therefore, this study aims to explore the anticancer effects of PA on SKOV-3 cells and to identify the potential apoptotic mechanism involved.

Materials and Methods

Chemical and reagents

The analytical grade chemicals and reagents were purchased from Sigma-Aldrich Chemical Co, United States and Nacalai, Japan.

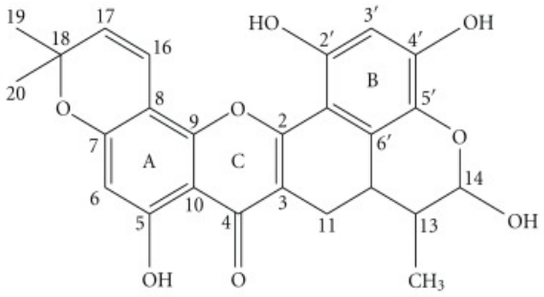

FIGURE 1. The chemical structure of PA

PA AND CONTROL DRUG PREPARATION

PA was obtained from the isolation of the stem bark of *Artocarpus obtusus* as previously described (Hashim et al. 2010). Dimethyl sulfoxide (DMSO) was used to dissolve the compound and control drug, with a maximum of 0.1 percent final concentration of DMSO in the final stock solution. The tested cell lines were given a two-fold series dilution concentration of PA and the control drug paclitaxel.

CELL CULTURE

Metastatic ovarian adenocarcinoma SKOV-3 cell line was acquired from the American Type Culture Collection (ATCC; Manassas, VA). The normal immortalized human ovarian surface epithelial cell line T1074 was originally purchased from Applied Biological Materials (abm®) Canada. SKOV-3 cells were cultured in McCoy's 5A medium and T1074 cells were cultured in Prigrow 1 medium. Both cultured cells were supplemented with 10% heat-inactivated foetal bovine serum (FBS), 100 u/mL of penicillin, 100 u/mL of streptomycin, and 20 mM of HEPES buffer at 37 °C in a humidified incubator in the presence of 5% CO_2 (Rahman et al. 2016).

CELL VIABILITY ASSAY

Following the harvest of confluence cells, the cells were centrifuged at 1,800 rpm for 5 min. The concentration of cells was, then, adjusted to 1×10^6 cells/mL. Then, the cells were treated with paclitaxel (control) and PA at various concentrations in a 96-well plate and incubated for 24, 48, and 72 h. About 20 µL of 3-(4,5-dimethylthiazol-2yl)-2,5-diphenyl tetrazolium bromide (MTT) reagent (Invitrogen, Carlsbad, USA) was added to each well and then, incubated for 3 h. The assay was carried out at an absorbance of 570 nm to determine the IC_{50} value.

SELECTIVITY INDEX ANALYSIS

The selectivity index (SI) of a drug or compound is a significant metric for determining a potential drug's ability to selectively kill cancer cells while being less toxic to healthy cells *in vitro* (López-Lázaro 2015). The SI was calculated using the following equation:

$$Selectivity\ Index = \frac{IC_{50\ calculated\ for\ normal\ cells}}{IC_{50\ calculated\ for\ cancer\ cells}}$$

APOPTOTIC MORPHOLOGICAL DUAL STAINING

The morphology of apoptosis was assessed using acridine orange (AO) and propidium iodide (PI) dual staining following the standard procedure. The examination was carried out under a fluorescent microscope (Leica, Wetzlar, Germany) attached to Q-Floro software. Briefly, a 25 mL culture flask (Nunc®, Sigma-Aldrich) was used for the assay. SKOV-3 cells were treated with the IC_{50} concentration of PA after being seeded at a density of 1×10^6 cells/mL. Then, the flasks were incubated for 24, 48, and 72 h at 37 °C. The harvested cells were later washed and then, stained with fluorescent dyes (AO/PI) comprising 10 µL (10 µg/mL) each of AO and PI. An ultraviolet fluorescent BX60 microscope (Olympus, Tokyo, Japan) was used to observe the cell morphology for 30 min before the disappearance of the fluorescence intensity. The categorization of healthy, apoptotic, and necrotic cells was carried out according to the literature (Kitazumi & Tsukahara 2011).

ANNEXIN-V-FITC ASSAY

A six-well plate was used to seed SKOV-3 cells (5×10^4 cells/mL). After exposure to PA for 24, 48, and 72 h, the cells were later harvested and then, washed with phosphate-buffered saline. A FITC (fluorescein isothiocyanate) Annexin V Apoptosis Detection Kit I

(BD Pharmingen™, San Diego, CA, USA) was used for the assay. The treated cells were first centrifuged at 1,600 rpm for 5 min. Then, 100 µL of each sample was taken and placed into a tube containing 5 µL of FITC Annexin V and 10 µL of PI stain. Following the mixing of the suspension, 100 µL of 1× assay buffer was added per tube prior to the analysis of all the samples using a flow cytometer (BD FACSCanto™ II, San Jose, CA, USA).

CELL CYCLE ANALYSIS

A T75cm^2 flask was used for SKOV-3 cells at a concentration of 5×10^5 cells and incubated overnight to allow attachment. The attached cells were treated with PA for 24, 48, and 72 h. Following the treatment, the cells were first trypsinized and then, centrifuged at 1,500 rpm for 10 min. The fresh pellets obtained were, then, washed twice with PBS, fixed with 500 µL of cold ethanol (70%), and incubated at −20 °C overnight. Following the removal of the remaining ethanol, the cells were resuspended in PBS containing 20 µL of RNase A (10 µg/mL) and 2 µL of PI (2.5 µg/mL). The resulting mixture was then incubated at 37 °C for 30 min in the dark. FACS Canto 11 Becton-Dickinson flow cytometry was used for immediate analysis of the samples (10,000 cells per sample). The percentage of cells at different phases was analysed using ModFit LT software (Verity Software House, Topsham, ME).

MULTIPLE CYTOTOXICITY 3 ASSAY

Cellomics® Multiparameter Cytotoxicity 3 kit (Thermo Scientific, Pittsburgh, PA, USA) was used for multiple cytotoxicity assays using a 96-well microplate. The concentration of cells in each well was 5×10^3 cells. Then, the cells were treated with PA for 24, 48 and 72 h and then, incubated overnight at 5% CO_2 saturation and 37 °C. Several solutions were then added successively to each well starting from 50 µL of live cell staining to 100 µL of fixation solution, 100 µL of 1× permeabilization buffer, and 100 µL of 1× blocking buffer for an incubation duration of 30, 20, 10, and 15 min. Two antibody solutions (primary and secondary antibody) were used (50 µL each) and added to the wells. An ArrayScan HCS reader was used to read the plate and evaluate the results.

REACTIVE OXYGEN SPECIES GENERATION ASSAY

The production of intracellular reactive oxygen species in PA-treated SKOV-3 cells was examined using 2′,7′-Dichlorofluorescin diacetate (DCFH-DA). The cells were first seeded in a 96-well black plate and then, incubated overnight to attach. Then, the cells were treated with PA for 24, 48, and 72 h. The cells were washed using Hank's balanced salt solution without serum. Then, 100 µL of DCFH-DA solution was added to each well prior to 30 min incubation at 37 °C. A fluorescence microplate reader (Tecan Infinite M 200 PRO, Männedorf, Switzerland) was used to analyse the results at 485 nm excitation and 520 nm emission.

ACTIVATION OF CASPASE-3, CASPASE-8 AND CASPASE-9 ASSAY

An R & D system kit (USA) was used to conduct the colorimetric assay of the activation of caspase-3, caspase-8, and caspase-9. Briefly, 90% confluent cells were induced in a T75cm^2 flask with PA for 24, 48, and 72 h. The induced cells were first trypsinized and then, centrifuged at 1,800 rpm for 10 min. Then, the fresh pellets were washed with cold PBS and lysed immediately with protein lysis buffer. The cell lysates were first kept on ice for 10 min, centrifuged at 10,000 g for 15 min, and then, transferred into a new tube. The fresh cell lysates (50 µL) containing 100–200 µg of protein was added to a 96-well plate in triplicate. Then, 50 µL of reaction buffer and 5 µL of caspase were then transferred into each well prior to incubation at 37 °C in a CO_2 incubator for 2 h. The analysis was carried out using a microplate reader (Tecan Infinite M 200 PRO, Männedorf, Switzerland) at 405 nm.

REAL-TIME PCR

The RNeasy Mini Kit was used to extract total RNA from SKOV-3 cells (Qiagen, Germany). A Nanodrop 2000 spectrophotometer was used to determine the final concentration of total RNA as well as its purity (Thermo Scientific). The 2-Step qRT-PCR Kit was used for RNA to cDNA conversion (Applied Biosystems, USA). In the gene expression assay, 1 µL of cDNA (at a concentration of 1 µg/mL) was combined with specific TaqMan primers and probes for the target genes, including β-actin, survivin, Bax, Bcl-2, HSP70, caspases-3, caspase-8, and caspase-9 (Applied Biosystems, USA). The gene expression levels were then measured with the StepOne Plus Real-time PCR System (Applied Biosystems, USA). The qRT-PCR cycling program typically involved cycling through 2 min of reverse transcription at 50 °C, followed by 20 s of initial polymerase activation at 95 °C. Subsequently, there was a 1 s denaturation step at 95 °C, and then 20 s of annealing

and extension at 60 °C. This entire cycle was repeated 40 times to amplify the target cDNA. Data analysis was performed using the comparative Ct (2-ΔΔCt) method to determine gene expression levels relative to reference genes or controls (Wong & Medrano 2005).

WESTERN BLOT

PA was exposed to SKOV-3 cells in a 75cm^2 culture flask for 24, 48, and 72 h. The total protein was extracted using lysis buffer (50 mM Tris–HCl, pH 8.0; 120 mM NaCl, 0.5% NP-40; and 1 mM PMSF). A BCA protein assay reagent kit (Bio-Rad, USA) was used to determine the protein concentration. Equal amounts of protein (40 µg) extract were subjected to SDS-PAGE and electroblotted onto a polyvinylidene difluoride membrane (Bio-Rad). Blots were then blocked with 5% non-fat milk in TBS-Tween buffer 7 (0.12 M Tris-base, 1.5 M NaCl, and 0.1% Tween 20) for 1 h at room temperature. Following incubation with the appropriate primary antibody overnight at 4 °C, the blots were first washed and later incubated with horseradish peroxidase-conjugated secondary antibody for 1 h at room temperature. The protein bands were detected using pico or Femto chemiluminescence (ECL system) and visualized using a UV gel documentation system. The subsequent primary antibodies including those for β-actin (1:1000) (Cat. No. ab8227), survivin (1:1000) (Cat. No. ab24479), Bax (1:1000) (Cat. No. ab32503), Bcl-2 (1:1000) (Cat. No. ab7973), HSP70 (1:1000) (Cat. No. ab45133), cleaved caspase -3 (1:10000) (Cat. No. ab32351), cleaved caspase -8 (1:10000) (Cat. No. ab25901) and cleaved caspase -9 (1:10000) (Cat. No. ab32539) were purchased from Abcam, Cambridge, United Kingdom.

HUMAN APOPTOSIS PROTEIN PROFILE ARRAY

The Proteom Profiler Array (RayBio® Human Apoptosis Antibody Array Kit, Raybiotech, USA) was used to determine the apoptosis-related proteins following the marker's instructions. The goal was to examine the pathways through which PA promotes apoptosis. The cells were treated with the IC_{50} values of PA for 48 h treatment. The treated cells were first lysed and then extracted. A total of 300 µg of proteins from each sample were incubated overnight. The data were obtained by scanning the membrane using a Biospectrum AC ChemiHR 40 (UVP, Upland, CA) and an examination of the file of the array image was conducted using image analysis software following the instruction of the company.

STATISTICAL ANALYSIS

All data were presented as means ± standard deviations (mean ± SD) and analysed using one-way ANOVA and post hoc Tukey HSD multiple comparison tests. Statistical analysis was carried out using the SPSS-16.0 software package and GraphPad prism 5.0, with $p<0.05$ considered significant.

RESULTS

PA SELECTIVELY INHIBITS THE PROLIFERATION OF SKOV-3 CELLS AND NORMAL CELLS

PA treatment resulted in a noticeable decrease in cell viability in SKOV-3 cells in a time-dependent fashion, with IC_{50} values of 7.0 ± 0.5 µg/mL observed after 72 h of treatment (Table 1). This compound exhibited a lesser effect on normal cells T1074 compared to the positive control, paclitaxel. The selectivity index analyses of PA and paclitaxel on SKOV-3 cells at different time points are also presented in Table 2. The selectivity index of PA increased over time and reached its highest value of 13.2 after 72 h of treatment.

PA SELECTIVELY INHIBITS THE PROLIFERATION OF SKOV-3 CELLS AND NORMAL CELLS

The morphological changes in SKOV-3 cells treated with PA were observed under normal inverted microscopy as shown in Figure 2. The dissociated morphological structure of the treated SKOV-3 cells was apparent after 24 h exposure to PA with the formation of apoptotic bodies. The marked reduction in the cell number was clearly visible, indicating that growth inhibition had occurred. However, the untreated SKOV-3 cells remained healthy with an intact structure.

PA INDUCES TIME-DEPENDENT APOPTOTIC MORPHOLOGICAL CHANGES IN SKOV-3

Figure 3 demonstrates that after 24 h of PA treatment, notable morphological changes were observed in SKOV-3 cells, signifying the onset of apoptosis. These changes encompassed membrane blebbing, cellular shrinkage, and nuclear alterations, all consistent with the early stages of apoptosis. The difference in apoptosis induction was statistically significant ($p<0.05$) in the treated cells. Furthermore, with extended exposure time (72 h after treatment), a concurrent increase in cell death, including secondary necrosis, was observed.

TABLE 1. The IC_{50} values of PA and paclitaxel on SKOV-3 and T1074 cells at different time points

Compounds/ Treatment period (h)	IC_{50} values at different time points (µg/mL)					
	SKOV-3			T1074		
	24	48	72	24	48	72
PA	10.0 ± 0.5	8.5 ± 0.5	7.0 ± 0.5	96.0 ± 0.5	90.5 ± 0.5	82.0 ± 0.28
Paclitaxel	4.6 ± 0.28	2.5 ± 0.2	0.8 ± 0.2	60.0 ± 0.5	49.5 ± 0.76	30.5 ± 0.5

TABLE 2. The selectivity index analysis of PA and paclitaxel on SKOV-3 cells at different time points

Compounds/ Treatment period (h)	SKOV-3 cells		
	24	48	72
PA	9.6	10.6	13.2
Paclitaxel	13.0	19.7	38.12

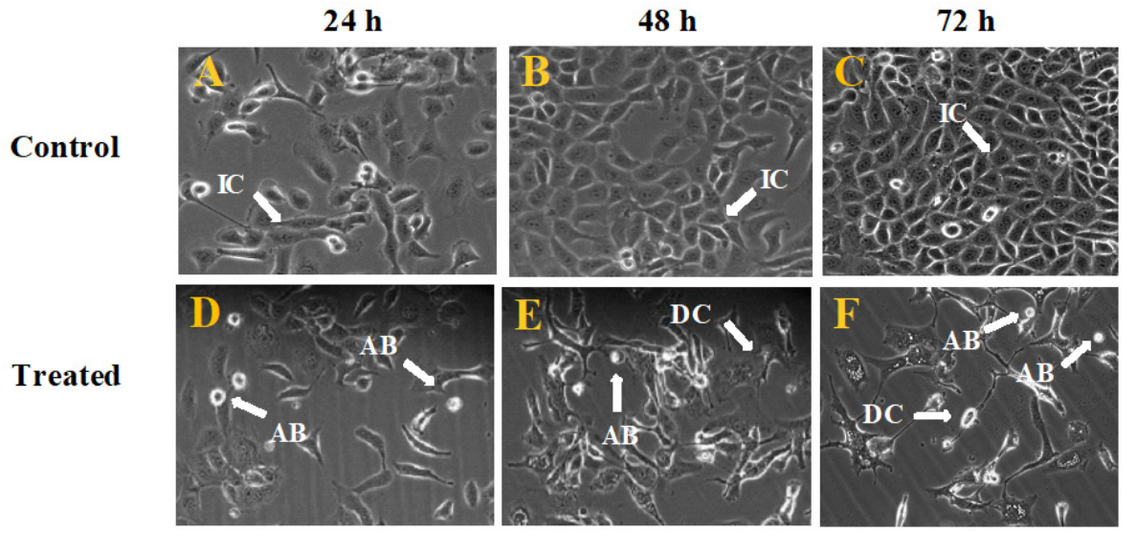

FIGURE 2. Microscopic evaluation of SKOV-3 cells treated with PA (8.5 µg/mL) at different time points (200× magnification). (A) Untreated cells 24 h. (B) Untreated cells 48 h. (C) Untreated cells 72 h. (D) Cells at 24 h treatment. (E) Cells at 48 h treatment. (F) Cells at 72 h treatment. IC: Intact cell structure; DC: dissociate cell structure and AB: apoptotic body

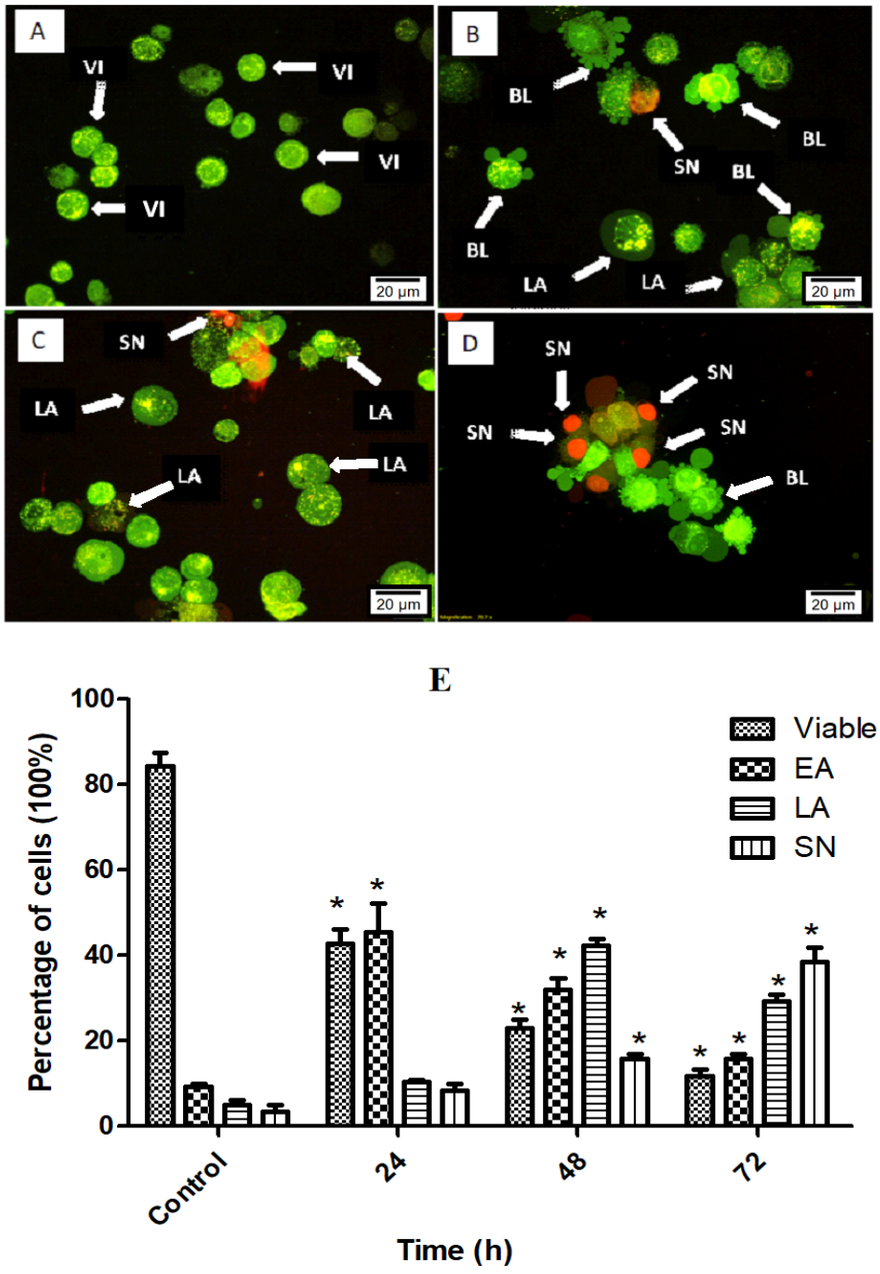

FIGURE 3. AOPI analysis of SKOV-3 cells treated with PA (8.5 µg/mL) at different time points. (A) Normal SKOV-3 cells. (B) SKOV-3 cells treated at 24 h. (C) SKOV-3 cells treated at 48 h. (D) SKOV-3 cells treated at 72 h. (E) Quantitative results of morphological cell changes at different time points. (EA: Cell at early apoptosis; LA: Cells at the late stage of apoptosis; and SN: Cell at secondary necrosis stage). Results are depicted as mean ± SD of three replicates. * Indicates a significant difference from the control of each phase ($p<0.05$)

PA TRIGGERS PHOSPHATIDYLSERINE EXPOSURE AND EARLY APOPTOSIS

The different kinetics of phosphatidylserine (PS) exposure on the plasma membrane's outer leaflet is one of the earliest biochemical changes in apoptosis events. Annexin V, a Ca^{2+}-dependent phospholipid-binding protein, has been shown to interact with PS specifically and strongly and can be used to detect apoptosis by targeting the loss of plasma membrane asymmetry. A significant increase in early apoptosis and late apoptosis was observed in SKOV-3 treated with PA at 24 h of treatment, which accounts for more than 50% of cells in apoptosis stages (Figure 4). After 48 and 72 h of continuous exposure to the PA, there was an increase in cells in the late apoptosis and necrotic region.

PA INDUCES S PHASE CELL CYCLE ARREST

The antiproliferative effect of PA regarding cell cycle arrest was evaluated using flow cytometry. As displayed in Figure 5, there was a time-dependent PA-induced depletion of SKOV-3 cells in the S phase. In the G0/G1 phase, however, there was a decrease in the proportion of cells despite the significant ($p<0.05$) increase in the accumulation of cells arrested at the S phase at 72 h. A significant increase ($p<0.05$) in the proportion of cells in the apoptosis phase was also observed.

PA TRIGGERS TIME-DEPENDENT REACTIVE OXYGEN SPECIES FORMATION

A time-dependent generation of intracellular reactive oxygen species (ROS) was significantly ($p<0.05$)

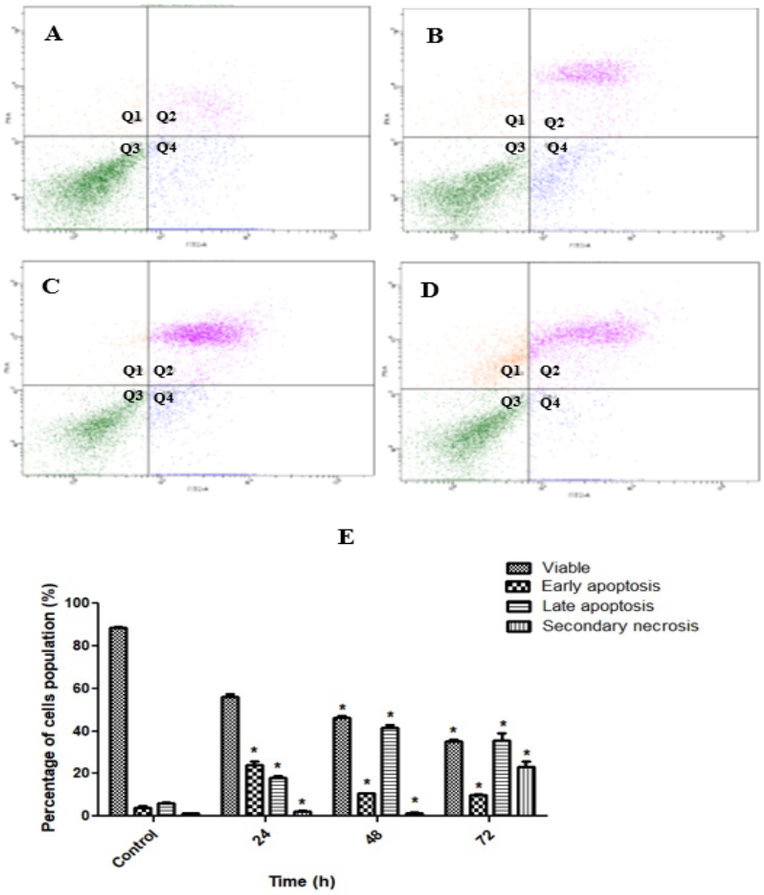

FIGURE 4. Annexin V-FITC flow cytometry assessment of SKOV-3 cells treated with PA (8.5 µg/mL) at different time points. The movement of the cell population commenced in Q3 (viable) to Q4 (early apoptosis) to Q2 (late apoptosis) and then to Q1 (secondary necrosis). [A] Control (untreated), [B] 24 h treatment, [C] 48 h treatment, and [D] 72 h treatment. [E] Histogram. Results are presented as mean ± SD of three replicates. *$p<0.05$ indicates a significant difference from the control

increased in SKOV-3 cells treated with PA as shown in Figure 6. At 24 and 48 h post-treatment, the treated cells displayed a 2-fold increase in the formation of ROS compared with untreated cells and decreased slightly after 72 h treatment.

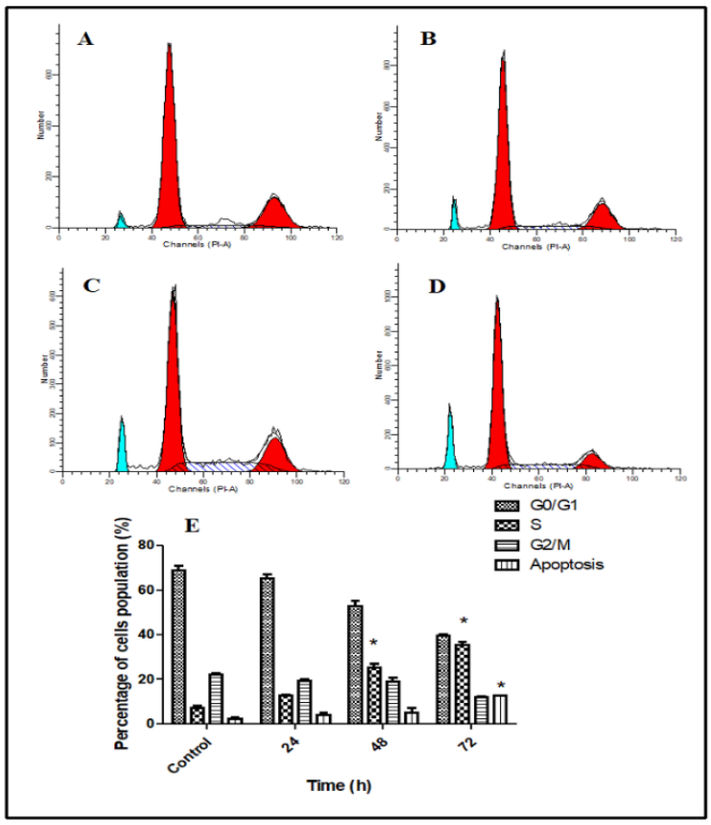

FIGURE 5. Cell cycle phase distribution analysis of SKOV-3 treated with PA (8.5 µg/mL) at different time points. [A] Control (untreated), [B] 24 h treatment, [C] 48 h treatment, and [D] 72 h treatment. [E] Histogram examination denoted cell cycle arrest in the S phase. Results are presented as mean ± SD of three replicates. *p<0.05 indicates a significant difference from the control

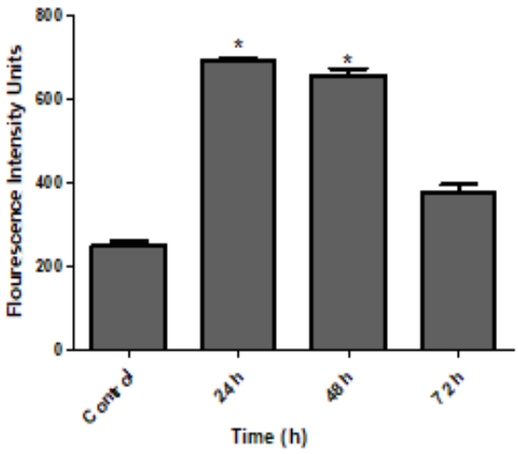

FIGURE 6. Effects of PA (8.5 µg/mL) on ROS generation in SKOV-3 cells. Cells were treated with PA for 24, 48, and 72 h. Values are expressed as mean ± SD from three independent experiments. Statistical significance was expressed as *p<0.05

PA TRIGGERS MITOCHONDRIAL DISRUPTION AND CYTOCHROME *c* RELEASE

For further investigation of the effect of PA on mitochondrial membrane potential (MMP) changes, cell permeability, cytochrome *c* localization and release from mitochondria, Hoechst staining and MMP fluorescence probe were used to evaluate the function of the nucleus and mitochondria. As shown in Figure 7, the decrease in both nuclear size and cell number due to exposure of SKOV-3 cells to PA was clearly visible. The treated cells exhibited clear nuclear condensation while the untreated SKOV-3 cells showed intact nuclei, as seen in Hoechst 33342 staining. The alterations in nuclear intensity, which are closely associated with apoptotic

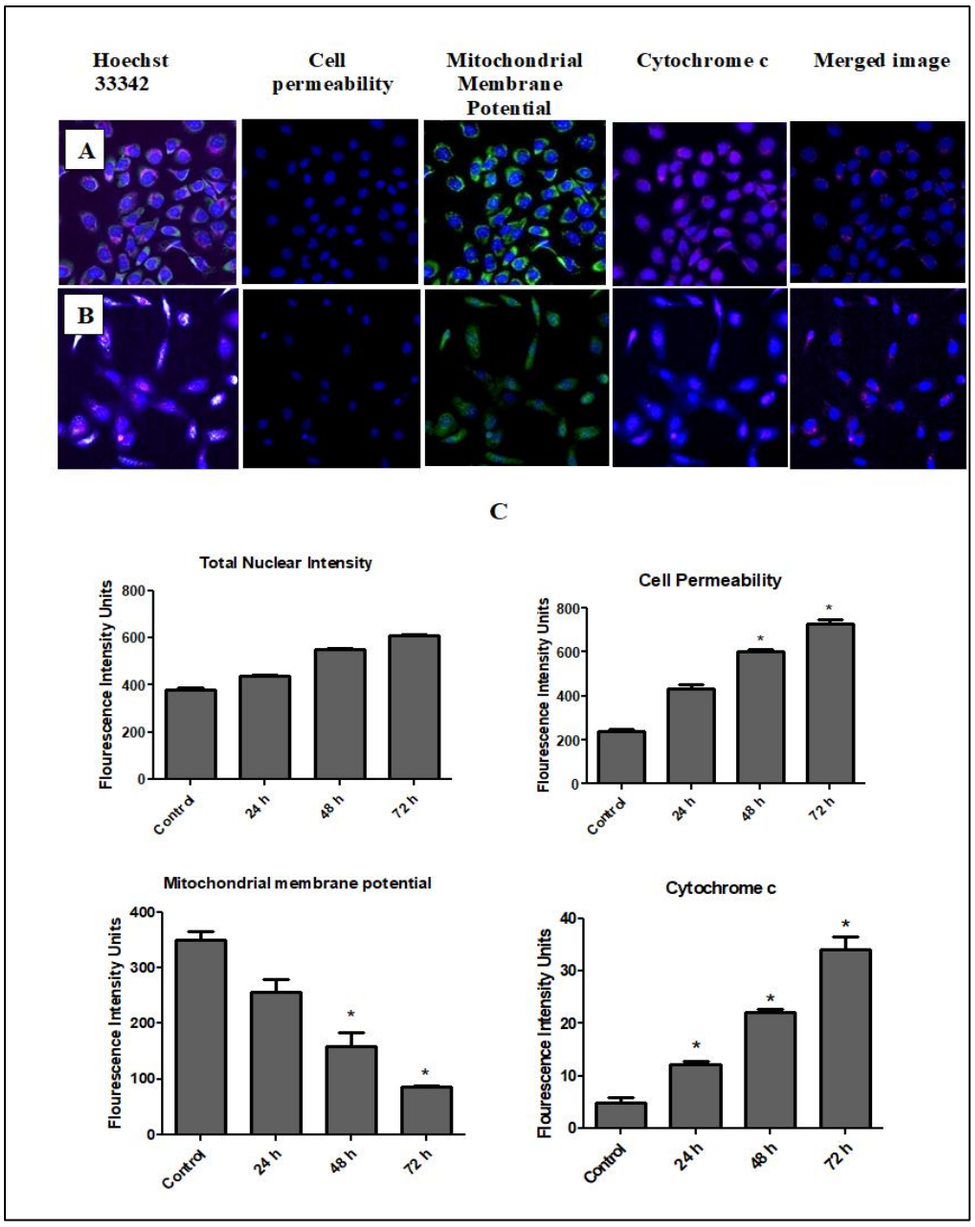

FIGURE 7. Illustrative image of SKOV-3 cells in a 96-well black plate exposed to either medium alone or 8.5 µg/mL PA for 24, 48, and 72 h. Images were observed at a magnification of 20×. (A) Untreated SKOV-3 cells and (B) SKOV-3 cells treated with 8.5 µg/mL of PA. (C) Time-dependent quantitative analysis of SKOV-3 cells treated with PA for different apoptosis parameters. Average intensities were observed simultaneously in SKOV-3 cells for total nuclear intensity, cell permeability, MMP, and cytochrome *c* release. All data were expressed as means ± SD. **p*<0.05 indicates a significant difference from the control

chromatin changes, such as membrane fragmentation, blebbing, and condensation, were quantified in Figure 7. Time-dependent increment in cell permeability upon SKOV-3 treatment was associated with a significant ($p<0.05$) reduction of green fluorescence intensity of MMP. These changes were also associated with the collapse of MMP. PA has been shown to elevate the highest translocation level of cytochrome *c* as early as 24 h treatment and decreased slightly after 48 and 72 h. The cyan fluorescence intensities of cytochrome c dye were markedly increased indicating the significant ($p<0.05$) cytochrome *c* release from mitochondria into the cytosol. The present findings exhibited a time-dependent significant ($p<0.05$) increase upon SKOV-3 treated with PA in total nuclear intensity, increased cell permeability, collapsed of MMP and elevated translocation of cytochrome *c* in the cytosol when compared to the control SKOV-3 cells.

PA INDUCES CASPASE ACTIVATION VIA INTRINSIC PATHWAY

Treatment of SKOV-3 cells with PA resulted in a significant ($p<0.05$) time-dependent activation of caspase-9 and caspase-3, as shown in Figure 8. The highest activation of caspase-9 was observed at 24 h of treatment, while the highest activation of caspase-3 was observed at 48 h. However, there was no significant increase ($p<0.05$) in the activation of caspase-8 throughout the treatment periods.

PA-INDUCED CHANGES IN APOPTOTIC MRNA EXPRESSION

Figure 9 illustrates the mRNA expression levels of Bax, Bcl-2, HSP70, survivin, caspase-3, caspase-8, and caspase-9 in untreated and PA-treated SKOV-3 cells. The expression levels of Bax, caspase-3, and caspase-9 increased significantly over time, with Bax and caspase-3 showing the highest upregulation, with 7-fold and 6-fold changes in mRNA levels after 72 h of treatment, respectively. Conversely, the expression levels of Bcl-2, survivin, and HSP70 genes were significantly *($p<0.05$)* down-regulated over time in PA-treated SKOV-cells.

WESTERN BLOT ANALYSIS

The Western blot analysis performed on SKOV-3 cells

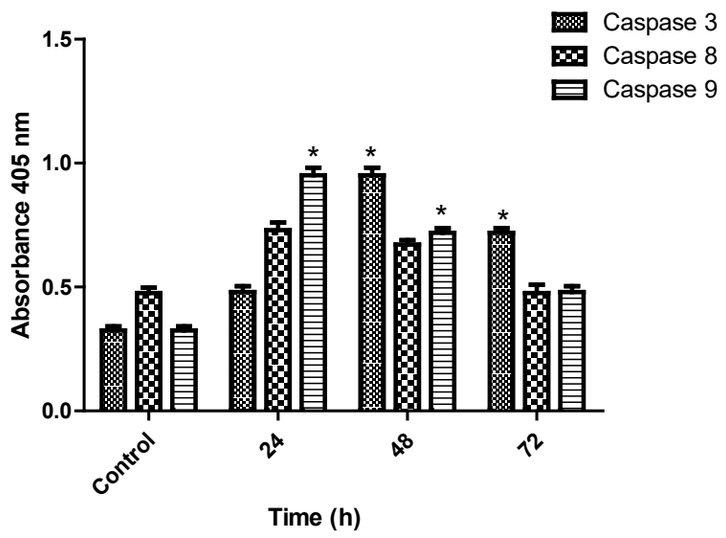

FIGURE 8. Effect of PA (8.5 µg/mL) on caspases activation at different time points. Results are represented as mean ± SD of three replicates. *$p<0.05$* indicates a significant difference from the control

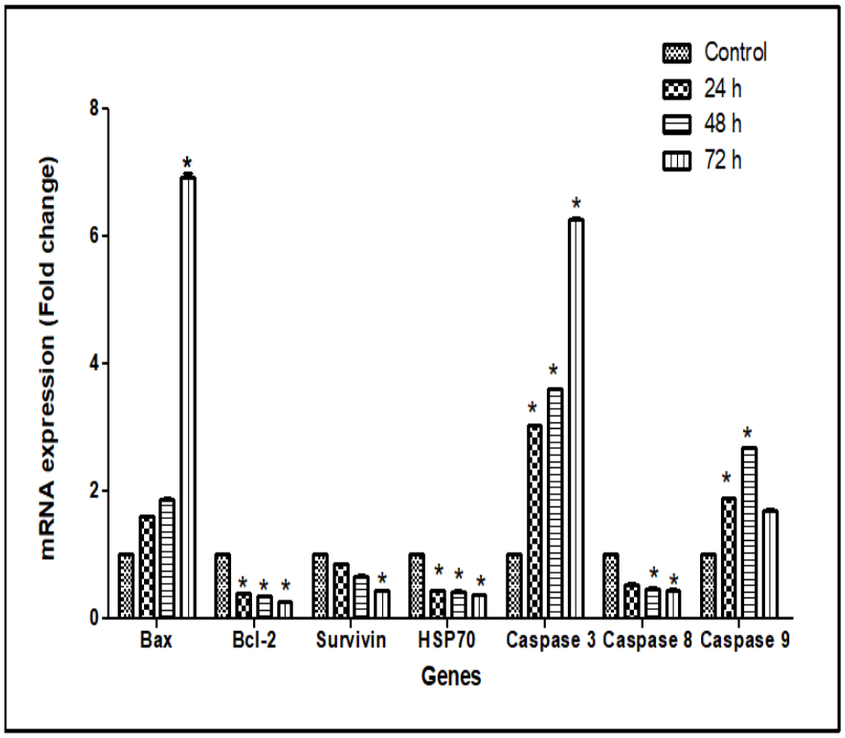

FIGURE 9. Effect of PA (8.5 µg/mL) on the mRNA expression of Bax, Bcl-2, Survivn, HSP70, Caspase 3, Caspase 8 and caspase 9 in SKOV-3 cells after 24, 48, and 72 h. β-Actin was used as a loading control. All data were expressed as mean ± SD. Statistical significance was expressed as $*p<0.05$

treated with PA showed a time-dependent upregulation of Bax, cleaved caspase-3, and cleaved caspase-9 proteins. The expression levels of cleaved caspase-3 and cleaved caspase-9 were significantly increased after 48 and 72 h of treatment. In addition, the expression levels of Bcl-2, survivin, HSP70, and cleaved caspase-8 were down-regulated in a time-dependent manner (Figure 10).

HUMAN APOPTOSIS PROTEIN PROFILE ARRAY

Figure 11 shows the results of an apoptosis protein profile assay that examined the expression levels of 43 apoptotic proteins in SKOV-3 cells treated with PA. The assay showed that 21 apoptotic proteins, including Bad, Bax, Bid, Bim, caspase-3, Cytochrome *c*, DR6, Fas, fasL, HTRA, IGFBP-3, IGFBP-4, p53, SMAC, sTNFRI, sTNFRII, TNF-α, TNF-β, TRAIL-R1, TRAIL-R2, TRAIL-R3, and TRAIL-R4, were upregulated in the treated cells. Among these, caspase-3, cytochrome *c*, DR6, FasL, HTRA, and TRAIL-R4 showed the highest levels of upregulation. On the other hand, 22 apoptotic proteins, including Bcl-2, Bcl-w, CD40, CD40L, cIAP-2, HSP27, HSP60, HSP70, IGF-1, IGF-2, IGFBP-1, IGFBP-2, IGFBP5, IGFBP6, IGF-1sR, livin, p21, p27, survivin, and Xiap, were down-regulated in the PA-treated SKOV-3 cells. Caspase-8 did not show any significant difference when compared to the control.

DISCUSSION

Our study uncovers the notable potential of PA, derived from the stem bark of *A. obtusus*, to exert a selective antiproliferative effect on SKOV-3 cells through the induction of apoptosis. It is noteworthy that while previous research has documented PA's ability to inhibit the proliferation of MCF7 cells (Mohan et al. 2012), there has been a dearth of information regarding its apoptotic actions specifically in SKOV-3 cells and the associated mechanisms. Thus, our investigation serves as a pioneering effort, establishing for the first time

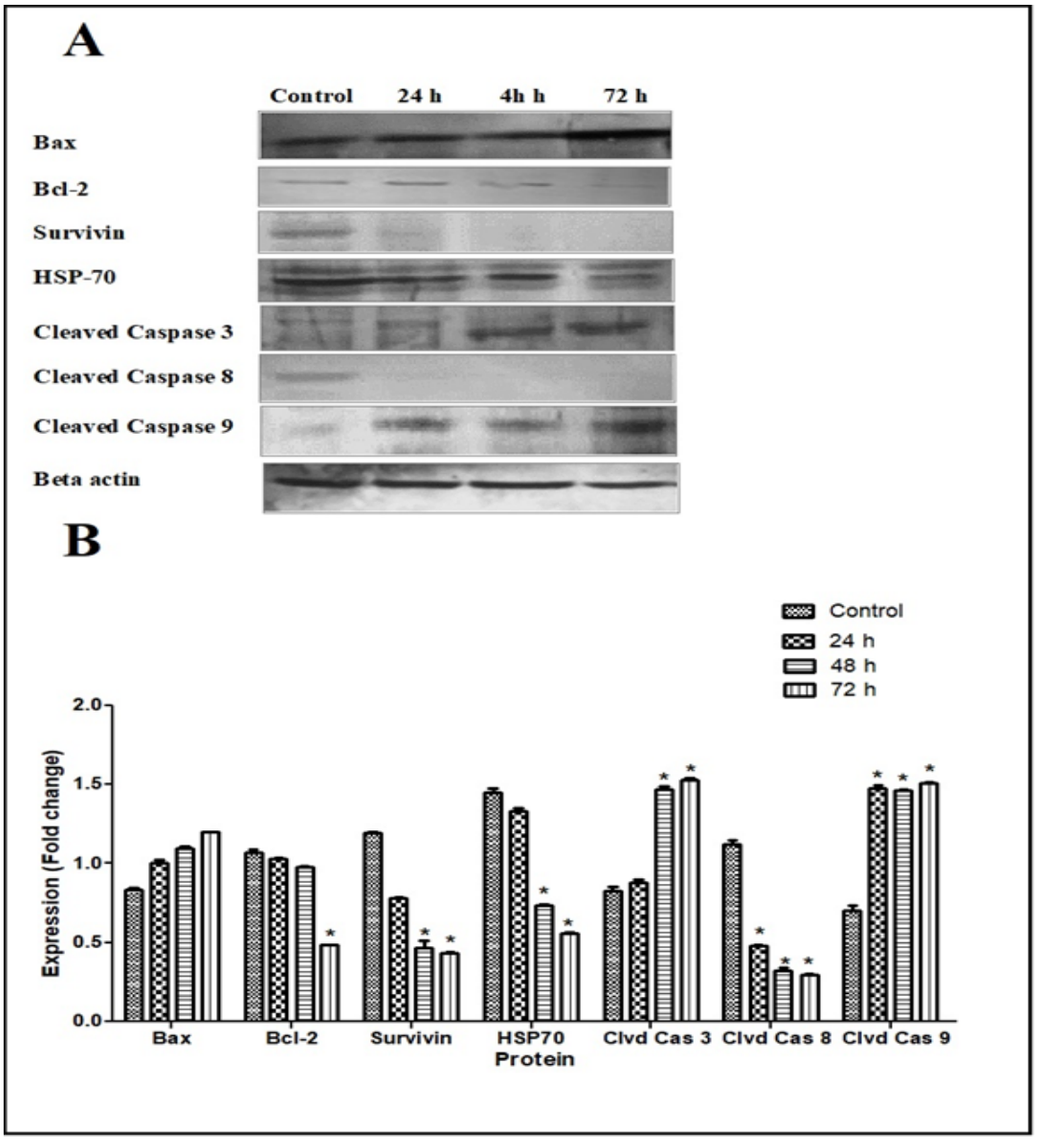

FIGURE 10. (A) Effect of PA (8.5 µg/mL) on the apoptosis protein expression after 24, 48, and 72 h. β-Actin was used as a loading control. (B) Quantitative analysis of SKOV-3 cells treated with PA. All data were expressed as mean ± SD. Statistical significance was expressed as $*p<0.05$

the apoptotic capabilities of PA against SKOV-3 cells, characterized by the mitochondria-dependent activation of the caspase cascade, heightened ROS levels, induction of S-phase cell cycle arrest, and modulation of Bcl-2 family proteins.

The adverse impact of existing chemotherapeutic drugs on both normal tissues and the development of drug resistance is a pressing concern affecting approximately 75% of ovarian cancer patients (Maleki et al. 2022). Consequently, there is an urgent demand for

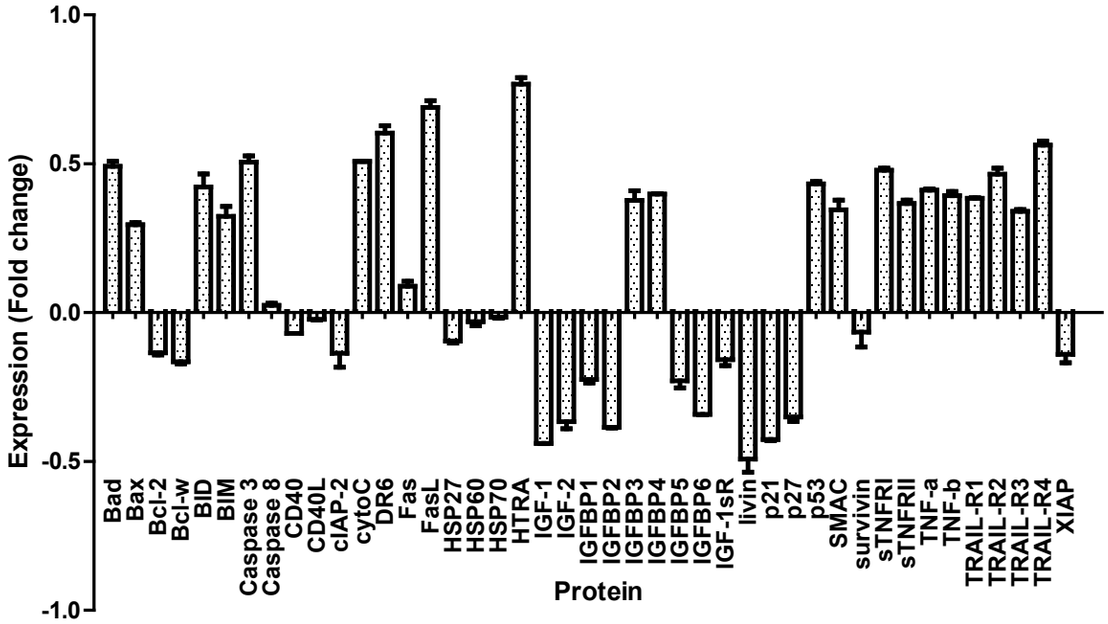

FIGURE 11. Human apoptosis proteome profile array in SKOV-3 cells treated with PA (8.5 μg/mL) at 48 h treatment with positive control signal as a housekeeping protein. The histogram represents a quantitative analysis of treated cells where the positive and negative fold changes indicate up and down-regulation of protein expression, respectively

the discovery of highly safe and effective agents that can mitigate drug side effects and combat drug resistance in advanced ovarian cancer (Teekaraman et al. 2019). In recent years, there has been growing interest in the potential of phytochemicals to influence mechanisms involved in tumorigenesis across various human malignancies (Hashemi et al. 2021; Lang et al. 2018). The primary objective of this study was to investigate the antiproliferative properties of xanthones, which may offer a safer alternative to current chemotherapy drugs, and to assess the role of PA as a potential anti-cancer agent against ovarian cancer cells. Furthermore, we aimed to unravel the underlying mechanisms responsible for their anti-cancer potential. Our findings align with previous research on artonin E, a prenylated flavonoid found in various *Artocapus* plants (Rahman & Hashim 2022).

In our study, we utilized the MTT assay to assess the impact of PA on the viability of SKOV-3 cells, which are derived from stage 3 ovarian cancer patients (Rasouli et al. 2021). SKOV-3 cells are notoriously resistant to various cytotoxic drugs, including tumour necrosis factors (Braga et al. 2020). Notably, our results demonstrated that PA induced a significant reduction in the viability of SKOV-3 cells, whereas normal human ovarian cell lines (T1074) exhibited lower susceptibility to PA-induced cytotoxicity. Achieving therapeutic selectivity is a paramount objective in drug discovery, as it helps mitigate the risk of non-specific toxicity and adverse side effects associated with many cytotoxic drugs.

Our findings indicate that PA possesses a higher selectivity index, comparable to that of the positive control drug paclitaxel. A higher selectivity index ratio suggests that a drug may potentially offer greater effectiveness and safety when administered *in vivo* (Calderón-Montaño et al. 2019). Importantly, this selective inhibition of SKOV-3 cells while sparing normal cells aligns with observations from other studies utilizing innovative approaches such as enzyme-instructed self-assembly and carbon quantum dots/Cu2O composite materials to target the cellular microenvironment (Chen et al. 2021; Li et al. 2017). This consistent pattern of selective inhibition against

highly resistant SKOV-3 cells, while preserving normal cell viability, underscores the promise of PA as a lead compound for potential anticancer therapy.

In the morphological evaluation of the mode of cell death induced by PA, the cell number decreased after prolonged exposure to PA as shown by normal inverted microscopy. The early and late phases of apoptosis in cells treated with PA were morphologically identified with AOPI double staining. In consistence with morphological results, the biochemical analysis using flow cytometry study also demonstrated that PA induces apoptosis in the early stage of apoptosis as detected by Annexin V-FITC. Annexin V and its conjugates are used to detect early apoptosis by binding specifically to exposed phosphatidylserine, a hallmark of this process (Worsley, Veale & Mayne 2022). Thus, the present findings suggest that PA induces apoptosis, as evidenced by apoptotic morphological alterations and early activation of biochemical apoptosis, as indicated by Annexin-V analysis.

ROS and mitochondria have recently received significant scientific attention due of their importance in apoptosis and cancer (Czabotar & Garcia-Saez 2023). Specifically, the apoptotic impact of PA on SKOV-3 cells is directly associated with increased intracellular ROS levels. This increase correlates with substantial enhancements in various cellular aspects, including total nuclear intensity, cell permeability, Mitochondrial Membrane Potential (MMP) levels, and the release of cytochrome *c* from mitochondria into the cytosol. Mitochondria serve as receivers of various signals, whether endogenous or external stimuli. The swift production of ROS can lead to the oxidative modification of mitochondrial pores, potentially disturbing the MMP and facilitating the translocation of cytochrome *c* from the mitochondria to the cytosol, ultimately promoting cell death. The results are in agreement with the literature where methotrexate also reportedly acts on SKOV-3 cancer cells, altering the MMP and causing DNA damage with apoptotic gene upregulation through an increase in intracellular ROS levels (Albasher et al. 2019). On the contrary, myricetin mechanistically reduced ROS levels in tumour cells and inhibited oxidative stress to suppress ovarian cancer (Li et al. 2022).

The process of cell division is tightly regulated, and any abnormalities in this process can lead to the development of cancer. One mechanism by which PA induces apoptosis in SKOV-3 cells appears to be through its effect on the cell cycle. Understanding the cell cycle in cancer is crucial for improving cancer treatment. In this study, it was observed that PA induces cell cycle arrest in the S phase. The S phase is a critical phase during which DNA synthesis occurs. Previous research has shown that inhibition of cyclin A-cdk2 during S phase leads to S phase arrest and apoptosis (Kim et al. 2022). When the cell activates cyclin-CDK-dependent transcription, it signals the decision to initiate a new round of cell division and enter S phase (Ditano, Sakurikar & Eastman 2021). Consequently, any compound or drug that induces S phase cell arrest can also cause apoptosis. Therefore, the findings of this study confirm that PA induces apoptosis and cell cycle arrest at the S phase in SKOV-3 cells.

This study explored the effectiveness of two common therapeutic strategies through stimulation of proapoptotic molecules and inhibition of antiapoptotic molecules. The results showed that proapoptotic molecules were stimulated by PA through caspase activation and modulation of Bcl-2 family proteins. The increased expression levels of caspases-9 and caspase-3 in this study suggests that PA induced apoptosis predominantly through mitochondria-mediated intrinsic pathway. In addition, the decrease in cleaved caspase-8 expression further supports the induction of apoptosis via the intrinsic pathway, as caspase-8 is typically involved in the extrinsic pathway of apoptosis (Green 2022).

The Bcl-2 family plays a central role in regulating apoptosis, encompassing both pro- and anti-apoptotic functions within the mitochondrial pathway (Czabotar & Garcia-Saez 2023). Our study demonstrated the prevention of apoptosis through the restoration of the Bcl-2/Bax balance in SKOV-3 cells treated with PA, as evidenced by the downregulation of Bcl-2 and upregulation of Bax protein. Notably, we observed a significant decrease *($p<0.05$)* in the expression of survivin and HSP70, essential components of the apoptosis inhibition pathway. This downregulation is of particular significance, given the well-established roles of survivin and HSP70 in promoting aggressiveness and drug resistance across various cancer types (Albakova et al. 2020; Wheatley & Altieri 2019; Zhang et al. 2022). These findings underscore the potential therapeutic implications of targeting these proteins in the context of cancer treatment. Furthermore, paclitaxel exhibited a similar effect by increasing the Bax/Bcl-2 ratio and inhibiting HSP27 expression, ultimately leading to hyperthermia-induced apoptosis (Kong et al. 2020). Inhibiting antiapoptotic molecules sensitizes cancer cells to proapoptotic signals, thereby inducing programmed cell death.

Conclusion

In summary, this study explored the potential of PA as an anti-cancer agent against metastatic ovarian cancer cells. The noteworthy feature of selectively targeting cancer cells while sparing normal cells underscores PA's promise as a leading candidate for future anticancer therapies. PA achieved this by inducing apoptosis in SKOV-3 cells through the mitochondria-mediated intrinsic pathway, involving ROS level elevation, cytochrome *c* release, caspase activation, and modulation of Bcl-2 family proteins. Additionally, PA caused S-phase cell cycle arrest, contributing to its overall anti-cancer effects. These findings contribute to the ongoing quest for safer and more effective alternatives to existing chemotherapeutic drugs in the treatment of advanced ovarian cancer.

Acknowledgements

The authors thank Universiti Malaya's Institute of Research Management and Monitoring for financial support (PPP-PG022-2014B) and the UMRG RP001C-13BIO, UM, and Faculty of Pharmacy for research facilities.

References

Albakova, Z., Armeev, G.A., Kanevskiy, L.M., Kovalenko, E.I. & Sapozhnikov, A.M. 2020. HSP70 multi-functionality in cancer. *Cells* 9(3): 587.

Albasher, G., AlKahtane, A.A., Alarifi, S., Ali, D., Alessia, M.S., Almeer, R.S., Abdel-Daim, M.M., Al-Sultan, N.K., Al-Qahtani, A.A., Ali, H. & Alkahtani, S. 2019. Methotrexate-induced apoptosis in human ovarian adenocarcinoma Skov-3 cells via ros-mediated Bax/Bcl-2-cyt-c release cascading. *OncoTargets and Therapy* 12: 21-30.

Braga, L.D.C., Gonçales, N.G., Furtado, R.D.S., Andrade, W.P.D., Silva, L.M. & Silva Filho, A.L.D. 2020. Apoptosis-related gene expression can predict the response of ovarian cancer cell lines to treatment with recombinant human trail alone or combined with cisplatin. *Clinics* 75: e1492.1-7.

Calderón-Montaño, J.M., Martínez-Sánchez, S.M., Burgos-Morón, E., Guillén-Mancina, E., Jiménez-Alonso, J.J., García, F., Aparicio, A. & López-Lázaro, M. 2019. Screening for selective anticancer activity of plants from Grazalema Natural Park, Spain. *Natural Product Research* 33(23): 3454-3458.

Chen, D., Li, B., Lei, T., Na, D., Nie, M., Yang, Y., Xie, C., He, Z. & Wang, J. 2021. Selective mediation of ovarian cancer SKOV3 cells death by pristine carbon quantum Dots/Cu_2O composite through targeting matrix metalloproteinases, angiogenic cytokines and cytoskeleton. *Journal of Nanobiotechnology* 19: 68.

Czabotar, P.E. & Garcia-Saez, A.J. 2023. Mechanisms of BCL-2 family proteins in mitochondrial apoptosis. *Nature Reviews Molecular Cell Biology* 24(10): 732-748.

Ditano, J.P., Sakurikar, N. & Eastman, A. 2021. Activation of CDC25A phosphatase is limited by CDK2/Cyclin A-mediated feedback inhibition. *Cell Cycle* 20(13): 1308-1319.

Gielecińska, A., Kciuk, M., Mujwar, S., Celik, I., Kołat, D., Kałuzińska-Kołat, Ż. & Kontek, R. 2023. Substances of natural origin in medicine: Plants vs. cancer. *Cells* 12(7): 986.

Green, D.R. 2022. Caspase activation and inhibition. *Cold Spring Harbor Perspectives in Biology* 14(8): a041020.

Hashemi, S.S., Amini-Farsani, Z., Rahmati, S., Jazaeri, A., Mohammadi-Samani, M. & Asgharzade, S. 2021. Oleuropein reduces cisplatin resistance in ovarian cancer by targeting apoptotic pathway regulators. *Life Sciences* 278: 119525.

Hashim, N.M., Rahmani, M., Ee, G.C.L., Sukari, M.A., Yahayu, M., Oktima, W., Ali, A.M. & Go, R. 2012. Antiproliferative activity of xanthones isolated from *Artocarpus obtusus*. *Journal of Biomedicine and Biotechnology* 2012: 130627.

Hashim, N.M., Rahmani, M., Sukari, M.A., Ali, A.M., Alitheen, N.B., Go, R. & Ismail, H.B.M. 2010. Two new xanthones from *Artocarpus obtusus*. *Journal of Asian Natural Products Research* 12(2): 106-112.

Ivanova, V., Dikov, T. & Dimitrova, N. 2017. Histologic subtypes of ovarian carcinoma: Selected diagnostic and classification problems in Bulgaria: Is low hospital volume an issue? *Tumori* 103(2): 148-154.

Joly, F., Fabbro, M., Follana, P., Lequesne, J., Medioni, J., Lesoin, A., Frenel, J-S., Abadie-Lacourtoisie, S., Floquet, A., Gladieff, L., You, B., Gavoille, C., Kalbacher, E., Briand, M., Brachet, P-E., Giffard, F., Weiswald, L-B., Just, P-A., Blanc-Fournier, C., Leconte, A., Clarisse, B., Leary, A. & Poulain, L. 2022. A phase II study of Navitoclax (ABT-263) as single agent in women heavily pretreated for recurrent epithelial ovarian cancer: The MONAVI – GINECO study. *Gynecologic Oncology* 165(1): 30-39.

Kim, I.H., Eom, T., Park, J.Y., Kim, H.J. & Nam, T.J. 2022. Dichloromethane fractions of *Calystegia soldanella* induce S-phase arrest and apoptosis in HT-29 human colorectal cancer cells. *Molecular Medicine Reports* 25(2): 60.

Kitazumi, I. & Tsukahara, M. 2011. Regulation of DNA fragmentation: The role of caspases and phosphorylation. *The FEBS Journal* 278(3): 427-441.

Kong, X.X., Jiang, S., Liu, T., Liu, G.F. & Dong, M. 2020. Paclitaxel increases sensitivity of SKOV3 cells to hyperthermia by inhibiting heat shock protein 27. *Biomedicine and Pharmacotherapy* 132: 110907.

Lang, F., Qu, J., Yin, H., Li, L., Zhi, Y., Liu, Y., Fang, Z. & Hao, E. 2018. Apoptotic cell death induced by Z-ligustilidein human ovarian cancer cells and role of NRF2. *Food and Chemical Toxicology* 121: 631-638.

Lathiff, S.M., Jemaon, N., Abdullah, S.A. & Jamil, S. 2015. Flavonoids from *Artocarpus anisophyllus* and their bioactivities. *Natural Products Communication* 10(3): 393-396.

Li, J., Shi, J., Medina, J.E., Zhou, J., Du, X., Wang, H., Yang, C., Liu, J., Yang, Z., Dinulescu, D.M. & Xu, B. 2017. Selectively inducing cancer cell death by intracellular enzyme-instructed self-assembly (EISA) of dipeptide derivatives. *Advanced Healthcare Materials* 6(15): 1601400.

Li, Q., Tan, Q., Ma, Y., Gu, Z. & Chen, S. 2022. Myricetin suppresses ovarian cancer *in vitro* by activating the P38/Sapla signaling pathway and suppressing intracellular oxidative stress. *Frontiers in Oncology* 12: 903394.

López-Lázaro, M. 2015. How many times should we screen a chemical library to discover an anticancer drug? *Drug Discovery Today* 2(20): 167-169.

Maleki, N., Yavari, N., Ebrahimi, M., Faisal Faiz, A., Khosh Ravesh, R., Sharbati, A., Panji, M., Lorian, K., Gravand, A., Abbasi, M., Abazari, O., Shafiee Mehr, M. & Eskandari, Y. 2022. Silibinin exerts anti-cancer activity on human ovarian cancer cells by increasing apoptosis and inhibiting epithelial-mesenchymal transition (EMT). *Gene* 823: 146275.

Marchetti, C., De Felice, F., Romito, A., Iacobelli, V., Sassu, C.M., Corrado, G., Ricci, C., Scambia, G. & Fagotti, A. 2021. Chemotherapy resistance in epithelial ovarian cancer: Mechanisms and emerging treatments. *Seminars in Cancer Biology* 77: 144-166.

Mohan, S., Abdelwahab, S.I., Kamalidehghan, B., Syam, S., May, K.S., Harmal, N.S.M., Shafifiyaz, N., Hadi, A.H.A., Hashim, N.M. & Rahmani, M. 2012. Involvement of NF-KB and Bcl2/Bax signaling pathways in the apoptosis of MCF7 cells induced by a xanthone compound Pyranocycloartobiloxanthone A. *Phytomedicine* 19(11): 1007-1015.

Nayak, M., Nagarajan, A., Majeed, M., Nagabhushanam, K. & Choudhury, A.K. 2018. *In vitro* anti-acne activity of phytoactives from the stem bark of *Artocarpus hirsutus* Lam. and characterisation of pyranocycloartobiloxanthone A as a mixture of two anomers. *Natural Product Research* 32(17): 2116-2120.

Pal, S., Bhowmick, S., Sharma, A., Sierra-Fonseca, J.A., Mondal, S., Afolabi, F. & Roy, D. 2023. Lymphatic vasculature in ovarian cancer. *Biochimica et Biophysica Acta (BBA) - Reviews on Cancer* 1878(5): 188950.

Pellegrini, E., Multari, G., Gallo, R.R., Vecchiotti, D., Zazzeroni, F., Condello, M. & Meschini, S. 2022. A natural product, voacamine, sensitizes paclitaxel-resistant human ovarian cancer cells. *Toxicology and Applied Pharmacology* 434: 115816.

Rahman, M.A., Ramli, F., Karimian, H., Dehghan, F., Nordin, N., Ali, H.M., Mohan, S. & Hashim, N.M. 2016. Artonin E induces apoptosis via mitochondrial dysregulation in SKOV-3 ovarian cancer cells. *PLoS ONE* 11(3): e0151466.

Rahman, M.A. & Hashim, N.M. 2022. Apoptotic induction mechanism of artonin E in 3D ovarian cancer cell lines. *Indonesian Journal of Pharmacy* 33(1): 147-158.

Rasouli, M., Mehdian, H., Hajisharifi, K., Amini, E., Ostrikov, K. & Robert, E. 2021. Plasma-activated medium induces apoptosis in chemotherapy-resistant ovarian cancer cells: High selectivity and synergy with carboplatin. *Plasma Processes and Polymers* 18(9): 2100074.

Schoutrop, E., Moyano-Galceran, L., Lheureux, S., Mattsson, J., Lehti, K., Dahlstrand, H. & Magalhaes, I. 2022. Molecular, cellular, and systemic aspects of epithelial ovarian cancer and its tumor microenvironment. *Seminars in Cancer Biology* 86: 207-223.

Sidahmed, H.M.A., Hashim, N.M., Amir, J., Abdulla, M.A., Hadi, A.H.A., Abdelwahab, S.I., Taha, M.M.E., Hassandarvish, P., Teh, X., Loke, M.F., Vadivelu, J., Rahmani, M. & Mohan, S. 2013. Pyranocycloartobiloxanthone A, a novel gastroprotective compound from *Artocarpus obtusus* Jarret, against ethanol-induced acute gastric ulcer *in vivo*. *Phytomedicine* 20(10): 834-843.

Singh, P. & Lim, B. 2022. Targeting apoptosis in cancer. *Current Oncology Reports* 24(3): 273-284.

Smirnova, I., Drăghici, G., Kazakova, O., Vlaia, L., Avram, S., Mioc, A., Mioc, M., Macaşoi, I., Dehelean, C., Voicu, A. & Şoica, C. 2022. Hollongdione arylidene derivatives induce antiproliferative activity against melanoma and breast cancer through pro-apoptotic and antiangiogenic mechanisms. *Bioorganic Chemistry* 119: 105535.

Teekaraman, D., Elayapillai, S.P., Viswanathan, M.P. & Jagadeesan, A. 2019. Quercetin inhibits human metastatic ovarian cancer cell growth and modulates components of the intrinsic apoptotic pathway in PA-1 cell line. *Chemico-Biological Interactions* 300: 91-100.

Wang, Z., Guo, B., Yue, S., Zhao, S., Meng, F. & Zhong, Z. 2022. HER-2-mediated nano-delivery of molecular targeted drug potently suppresses orthotopic epithelial ovarian cancer and metastasis. *International Journal of Pharmaceutics* 625: 122126.

Wheatley, S.P. & Altieri, D.C. 2019. Survivin at a glance. *Journal of Cell Science* 132(7): p.jcs223826.

Wong, M.L. & Medrano, J.F. 2005. Real-time PCR for mRNA quantitation. *BioTechniques* 39(1): 75-85.

Worsley, C.M., Veale, R.B. & Mayne, E.S. 2022. Inducing apoptosis using chemical treatment and acidic pH and detecting it using the annexin V flow cytometric assay. *PLoS ONE* 17(6): e0270599.

Wu, G., Peng, H., Tang, M., Yang, M., Wang, J., Hu, Y., Li, Z., Li, J., Li, Z. & Song, L. 2021. ZNF711 down-regulation promotes cisplatin resistance in epithelial ovarian cancer via interacting with JHDM2A and suppressing SLC31A1 expression. *EBioMedicine* 71: 103558.

Yeung, T.L., Leung, C.S., Yip, K.P., Au Yeung, C.L., Wong, S.T. & Mok, S.C. 2015. Cellular and molecular processes in ovarian cancer metastasis. *American Journal of Physiology - Cell Physiology* 309(7): C444-C456.

Zhang, H., Gong, W., Wu, S. & Perrett, S. 2022. Hsp70 in redox homeostasis. *Cells* 11(5): 829.

*Corresponding author; email: najihahmh@um.edu.my